

AR/Int. P Sep/63-5  
31st May, 1963

A COMPUTER STUDY OF THE MUON CONTAMINATION  
IN THE RF VERSION OF THE O2 BEAM

by

E. Keil

1. Introduction
2. Theory of Muon Contamination
3. Numerical Procedure
4. Results
5. Acknowledgements
6. References.

## 1. Introduction

The ratio of the pion flux and the K or  $\bar{p}$  flux obtained from the CPS is, according to present estimates <sup>1)</sup>, between 100 and 1000 for momenta between 10 and 15 GeV/c. This makes the muon contamination a rather serious problem in beams like the RF version of the O2 beam which aims at the separation of K's and  $\bar{p}$ 's from  $\pi$ 's in that momentum range. The fraction of decay muons entering the NBBC must be very small indeed to obtain these beams with reasonable purity.

Rough estimates based on the fraction of pions decaying and on the momentum bite passing the final momentum analyser yield muon numbers exceeding the number of K's or  $\bar{p}$ 's. At the same time, various physical arguments which cannot easily be fitted into a simple theory lead to the conclusion that the rough estimates must be appreciably higher than the true figures. So there is a strong incentive to make better estimates.

The present report describes some computer studies of the muon contamination that were done with a slightly modified version of an existing programme. <sup>2)</sup>

## 2. Theory of Muon Contamination

### 2.1 General formula

We call  $W(p,q,z) dq dz$  the probability that a muon with a momentum between  $q$  and  $q + dq$  produced between  $z$  and  $z + dz$  metres from the target contaminates a beam tuned to the momentum  $p$  of the pions.

This function  $W$  can immediately be split into 4 factors:

$$W(p,q,z) = S(p,q) T(p,q,z) U(p,z) V(p,z) \quad (1)$$

where the factors have the following physical significance.  $U$  and  $V$  come from the fact that, for two reasons, the number of pions is not constant along the beam. Collimators may intercept some fraction of the pion beam. This is taken into account by the factor  $U(p,z)$  which may decrease when passing through a collimator or another aperture limitation but is constant elsewhere. It seems advisable to normalize the pion number at the end of the beam where it is well defined. Then  $U(p,z)$  is the ratio of the phase space area at a distance  $z$  to that part of this area that reaches the end of the beam. With this definition  $U = 1$  in a beam from the last beam defining collimator onwards.

The decay of the pions leads to a continuous decrease of their number and of the probability  $V(p,z) dz$  that they decay between  $z$  and  $z + dz$ . Taking the proper normalisation at the end of the beam

$$V(p,z) dz = \frac{dz}{\lambda} \exp \left[ -(L - z)/\lambda \right] \quad (2)$$

$\lambda$  is the mean free path of the pion

$$\lambda = 54.76 p \quad [m] \quad (3)$$

where  $p$  is in GeV/c, and  $L$  is the length of the beam.

The remaining two functions deal with the muon.

$S(p, q) dq$  is the probability that a decaying pion of momentum  $p$  decays into a muon with a momentum between  $q$  and  $q + dq$ .  $S$  is a very simple function as the momentum distribution of the muons is uniform for  $0.573p \leq q \leq p$ . Thus

$$S(p, q) = \begin{cases} 1/(0.427p) & \text{for } 0.573p \leq q \leq p \\ 0 & \text{for } 0 \leq q < 0.573p \end{cases} \quad (4)$$

The  $p$  in the denominator enters since the definition of  $S$  is based on absolute rather than relative momentum bites.

Finally,  $T(p, q, z)$  gives the probability that the decay muon originating at the distance  $z$  and having the momentum  $q$  reaches the end of the beam.

By combining (1), (2), (4) one obtains:

$$W(p, q, z) dq dz = U(p, z) T(p, q, z) \frac{\exp[-(L-z)/\lambda]}{0.427 \lambda p} dq dz \quad (5)$$

If one integrates this expression over  $z$ , one obtains the muon spectrum  $M$ :

$$M(p, q) dq = dq \int_0^L W(p, q, z) dz \quad (6)$$

$M(p, q) dq$  is the number of muons with momenta between  $q$  and  $q + dq$  arriving at the end of the beam for one pion with momentum  $p$  arriving there.

Integration of  $M$  over  $q$  yields the contamination  $C$  defined as the total number of muons arriving at the end of the beam for one pion:

$$C(p) = \int_{0.573p}^p M(p, q) dq$$

The theory presented so far assumes a  $\delta$ -function as pion spectrum. This is certainly not true in practice, where all pion momenta are present according to their production rates up to the momentum slit, and pions inside a small momentum bite behind this slit. So, in principle, one should, at a given tuning of the beam, perform another integration over the actual pion momentum weighting them according to their contribution to the beam in various places.

However, this step was omitted to simplify the computations. It seems justified by the following two reasons:

- i) The momentum distribution of the pions behind the momentum slit is rather narrower than the muon spectrum.
- ii) The momentum slit is rather near to the target. Thus the fraction of path length where the decay of pions with completely wrong momentum can contaminate the beam is also rather small.

## 2.2 Simple approximate formula

Assuming that  $U = 1$ , and replacing  $T$  by some average value  $\bar{T}(p,q)$ , one can perform the  $z$ -integration analytically.

$$M(p,q) = \frac{\bar{T}(p,q)}{0.427 p} \exp(L/\lambda) [1 - \exp(-L/\lambda)] \quad (8)$$

The factor in the bracket is the fraction of pions decaying. Using the mean value theorem

$$\int \bar{T}(p,q) dq = \langle T(p) \rangle \Delta q \quad (9)$$

one gets the following simple formula:

$$C(p) = 2.34 \langle T(p) \rangle \exp(L/\lambda) [1 - \exp(-L/\lambda)] (\Delta q/p) \quad (10)$$

If one has found approximate values of  $\langle T(p) \rangle$  and of  $\Delta q$  simply, one can use (10) for a quick rough estimate.

One obtains the upper limit mentioned in the introduction by putting  $\langle T(p) \rangle = 1$ .

### 3. Numerical procedure

#### 3.1 Computation of $U(p, z)$

Comparing the definition of  $U(p, z)$  given in 2.1 and the definition given in <sup>2)</sup> for the transmission of primary particles, one concludes:

$$U(p, z) = 1/\tau(p, z) \quad (11)$$

Thus in order to obtain  $U$ , one must simply compute  $\tau$  at the pion momentum along the whole beam and take the reciprocal. These values are automatically correct after the first horizontal and vertical collimators. In front of them the  $\tau$  is taken relative to phase areas assumed in the programme. By an appropriate choice one can take into account other aperture limitations such as the PS vacuum chamber or the iron beam pipe. Thus  $\tau$  should also be approximately correct at the beginning of the beam. Table 1 gives  $U(p, z)$ . As only pions at the design momentum of the beam are considered,  $U$  is independent of  $p$ .

Table 1:  $U(p, z)$

$z$ (m)	$U(p, z)$
$0 \leq z \leq 7.68$	2.93543
$7.68 < z \leq 8.6$	1.91109
$8.6 < z \leq 34.3$	1.33332
$34.3 < z$	1

### 3.2 Computation of $T(p,q,z)$

The definition of  $T(p,q,z)$  given in 2.1 is chosen such that it agrees with the definition of the "taux moyen" used in <sup>2)</sup> for the muons from decay in flight of pions. So the whole  $T$  computation can also be done with this programme.

It assumes that all diaphragms absorb all particles hitting them, which is certainly not true in practice. But the energy loss corresponding to the full length of the collimators (50 cm copper) reduces the particle momentum such that they are eliminated by the final momentum analyser. Furthermore, the shape of the collimator jaws makes it rather improbable that particles travel only a short distance in the jaws and then come out again.

### 3.3 Computation of Muon Spectra and Contamination

All the functions appearing in the integrals for the muon spectrum (6) and for the overall contamination (7) are now known. The necessary integrations must be done numerically.

The actual treatment of the numerical results for the two cases considered

- i) "pion beams"
- ii) "separated beams"

is described in the following sections.

#### 3.3.1 Contamination of Pion Beams

What we call a pion beam here is a beam where the beam stopper is replaced by a collimator of the same width. The computation of the muon contamination in this beam is quite straightforward from the information given so far. As pion beams are only an intermediate stage in the present exercise, the pion decay is stopped at the beam stopper. Thus the contamination due to decay after the beam stopper is not taken into

account. As in this part of the beam the elimination of muons with wrong momentum is much less efficient than elsewhere, a substantial contribution to the whole contamination will come from this region.

### 3.3.2 Contamination of "Separated Beams"

In a "separated beam" the central part is stopped by a beam stopper; particles can only get through slits above and below it. The contamination in such a beam can be computed as the difference of two openings of a slit at the position of the beam stopper, as indicated in Fig. 1.

This procedure gives indeed the right answer as the two RF cavities will usually be phased such that their deflections cancel for the pions. Proceeding this way one neglects the difference of the deflections of pions and muons. This is justified at least at the higher momenta where their velocity difference is small. The advance  $\varphi$  in RF phase of the muons with respect to the pions varies linearly from 0 if the decay happens after the centre of the second cavity up to an upper limit if the decay takes place in front of the first one.

One finds:

$$\varphi = 1.5 L/(p^2 \lambda) \quad \text{degrees} \quad (12)$$

where  $L$  in metres is the distance from the decay point to the second cavity ( $L \leq 50$  m),  $p$  is the momentum in GeV/c, and  $\lambda$  is the RF wavelength.

This error in phase  $\varphi$  has the same influence as an accidental phase error in the phasing system. Both can be treated with the same methods. Reading formula (10) in <sup>3)</sup> backwards and neglecting the sine term, one obtains for the increase in beam stopper radius  $r$  necessary to allow for a phase error  $\varphi$  :

$$\delta r/r = 0.039 \varphi \quad (13)$$



where  $\varphi$  is in degrees. Combining this with (12) one gets:

$$\delta r/r = 0.06 L/(\lambda p^2) \quad (14)$$

Thus at  $p = 15 \text{ GeV}/c$ , the increase in beam stopper radius is 13% which is almost within the tolerances assumed in <sup>3)</sup>. As  $p = 5 \text{ GeV}/c$ ,  $\delta r/r = 1.2$ . This means that in order to allow for the phase error of the muons one must increase the beam stopper radius such that more than 50% of the wanted particles are lost. This is however not serious, as there is more intensity available at lower momenta.

#### 4. Results

The actual computer studies were carried out for the RF version of the O2 beam. The optical details of this beam are described elsewhere <sup>1) 4)</sup>. Here we only give the apertures of the collimators used for the different cases studied.

Table 1: Collimator Apertures [mm]

Aperture	"normal" purity		high purity	
	pion beam	separated beam	pion beam	separated beam
C1	$\pm 25$	$\pm 25$	$\pm 25$	$\pm 25$
C2	$\pm 60$	$\pm 60$	$\pm 30$	$\pm 30$
C3	$\pm 3$	$\pm 3$	$\pm 3$	$\pm 3$
C4	$\pm 5$	$\pm 5$	$\pm 5$	$\pm 5$
C5	$\pm 5$	$\pm 5$	$\pm 5$	$\pm 5$
beam stopper	$\pm 9$	$\pm (27-9)$	$\pm 9$	$\pm (27-9)$
C7	$\pm 90$	$\pm 90$	$\pm 90$	$\pm 90$
C8	$\pm 32$	$\pm 32$	$\pm 16$	$\pm 16$
C9	$\pm 14$	$\pm 14$	$\pm 14$	$\pm 14$
C10	$\pm 7$	$\pm 7$	$\pm 7$	$\pm 7$
pulsed magnet	$\pm 40$	$\pm 40$	$\pm 40$	$\pm 40$
BMS	$\pm 20$	$\pm 20$	$\pm 5$	$\pm 5$

Most of the results are given for pion momenta of 5 and 15 GeV/c. These values seem to be the practical limits of operation for an RF separator in the O2 beam, for the following two reasons:

- i) Above 15 GeV/c the particle flux becomes too small.
- ii) Below 5 GeV/c the ratio  $K^-/\pi^-$  becomes so small that the contamination exceeds tolerable limits.

Between 5 and 15 GeV/c the contamination is always smaller than at the ends.

#### 4.1 Pion Beams

##### 4.1.1 "Muon Sources" in Pion Beams

Figs. 2 and 3 show  $U(z) T(p, q, z)$  for  $p = 15$  GeV/c and 5 GeV/c respectively as a function of  $z$  for various  $q$ . This function essentially gives the contribution of different places in the beam to the muon flux with momentum  $q$ .

For  $q = p$  the probability that a muon gets into the bubble chamber is practically 100% all along the beam, except in a few places where the beam is very wide. There the divergence is so small that even the small production angle of the muon makes it sometimes miss the acceptance. As the production angle is slightly higher at  $p = 15$  GeV/c, the minima are slightly more pronounced there.

With decreasing  $q$  the minima in the probability function become more and more marked. These muons come almost entirely from the vicinity of the images. Of course, this effect is more obvious at  $p = 5$  GeV/c where the production angles for muons with  $q < p$  are much higher.

These facts were already known before <sup>5)</sup>. They were the reason for designing the electrostatic version of the O2 beam with non-coinciding images and formed the basis of an approximate contamination formula.

The detailed computation now shows that the strong peaking applies only to muons that could be eliminated with a good momentum analyser.

It also shows the order of magnitude of image separation necessary to suppress the maxima. Although the first images around 30 m are separated by 4 m there is almost no suppression visible for the acceptance used here.

#### 4.1.2 Muon Spectra

Figs. 4 and 5 show the muon spectra for  $p = 5$  and  $15$  GeV/c. As one would already expect from a comparison of Figs. 2 and 3, the muon spectrum at  $p = 5$  GeV/c is much more peaked at  $q = p$  than the other one. This indicates that it is more difficult to remove the muons from a 5 GeV/c beam than from a 15 GeV/c beam. Table 2 gives the relative widths of the two spectra:

Table 2: Widths of Muon Spectra

$p$ [GeV/c]	$\langle p-q \rangle / p$
5	0.603%
15	1.774%

#### 4.1.3 Muon Contamination of Pion Beams

Two main effects vary the muon contamination in different directions when reducing the pion momentum:

- i) The reduced decay length of the pions increases the number of muons produced.
- ii) The increased average production angle of the muons reduces their chance to stay inside the acceptance of the rest of the beam.

Table 3 shows that in actual fact both effects nearly cancel their influence on the contamination of pion beams.

Table 3: Muon Contamination of Pion Beams

p [GeV/c]	C (p)
5	$0.783 \times 10^{-2}$
15	$0.725 \times 10^{-2}$

Both these values are quite within tolerable limits. In this respect one should of course remember the remark made in 3.3.

#### 4.2 Separated Beams

##### 4.2.1 "Muon Sources" in Separated Beams

Figs. 6 and 7 show  $U(z)$   $T(p,q,z)$  for  $p = 5$  and  $15$  GeV/c.

For  $q = p$  the maxima of the pion beams are now minima of the separated beams as one would expect. But already at  $q = 0.99 p$  the peaks start occurring near the images; this effect is again more pronounced at  $p = 5$  GeV/c.

##### 4.2.2 Muon Spectra of Separated Beams

Figs. 8 and 9 show the muon spectra at  $p = 5$  and  $15$  GeV/c respectively. One can see quite marked differences.

As a separated beam accepts particles just outside the initial phase area in the vertical plane, a higher contamination must be expected at the lower momentum where the decay angles are higher.

For the same reason there is an extended minimum in the  $15$  GeV/c plot whereas in the other case only the  $q = p$  case drops below the others. This is even better seen on Fig. 10 showing  $(M_2 - M_1)/M_2$ , the fraction

of muons missing the beam stopper. For  $p = 15 \text{ GeV/c}$  this fraction has two distinct levels where it is roughly constant and quite a small transition region; for  $p = 5 \text{ GeV/c}$  one can only see the transition region.

The  $p = 15 \text{ GeV/c}$  curve confirms the assumption that the muons with small momentum errors behave so much like pions that almost all of them are caught by the beam stopper. With increasing width of the beam stopper, one should expect that the transmitted fraction goes down and that the transition region is shifted to lower momenta.

#### 4.2.3 Muon Contamination of Separated Beams.

As was already said before, particles outside the initial phase area are accepted in separated beam. Thus the two effects that cancelled for pion beams (4.1.3) now both tend to increase the contamination at lower momenta. Table 4 gives the computed numbers.

Table 4: Muon Contamination of Separated Beams

$p \text{ [ GeV/c ]}$	$C(p)$	$\mu^-/K^-$
5	$0.279 \times 10^{-2}$	5.6
15	$0.32 \times 10^{-3}$	0.16

The ratio  $\pi^-/K^-$  is roughly 2,000 at 5 GeV/c, and 500 at 15 GeV/c<sup>1)</sup>. Multiplying  $C(p)$  with these numbers, one obtains the ratio  $\mu^-/K^-$  also given in Table 4.

The purity obtained for the 15 GeV/c beam is rather satisfactory whereas a 5 GeV/c  $K^-$ -beam with the setting of the collimators chosen is clearly excluded.

However, the  $K^-$  flux at 5 GeV/c is 25 times higher than at 15 GeV/c <sup>1)</sup>. Therefore beams at this momentum need much less acceptance and can be designed for high purity. An attempt in this direction shall be described in the following section 4.3.

#### 4.3 "High Purity" Beam

With the setting of the collimators chosen for the computations done so far, the resolution of the final momentum analyser is rather poor, as can be seen from Fig. 11.

This poor resolution is due to the fact, that the entrance slit of this momentum analyser C8 sits on a rather wide image of C2, and that the exit slit formed by the gap of M8 is also rather wide <sup>4)</sup>. This solution was chosen since the lack of flight path made producing an image of the target in C8 impossible.

If one wants to improve the resolution, one must close down C2, C8 and M8. As C2 is the horizontal divergence defining slit, the accepted solid angle is reduced at the same time.

As an example the "high purity" settings given in Table 1 were used. Fig. 11 shows the improved resolution that can be obtained in this way. Figs. 12 and 13 show the muon spectra of the pion beam and the separated beam respectively. The overall muon contamination is given in Table 5.

Table 5: Muon Contamination in a high purity beam at  $p = 5$  GeV/c

beam	$c(p)$	$\mu^-/K^-$
pion	$0.487 \times 10^{-2}$	-
separated	$0.102 \times 10^{-2}$	2.04

The purity obtained is still not satisfactory.

The shapes of the transmission curve in Fig. 11 and the muon spectrum in Fig. 13 are roughly identical. Thus any further improvement in purity can only be proportional to the improvement in resolution, obtained by further reduction in the accepted solid angle.

The ratio  $\pi^-/K^-$  goes down from 2,000 at 5 GeV/c to 350 at 8 GeV/c<sup>1)</sup>. Thus, even with constant  $C(p)$  for separated beams, the ratio  $\mu^-/K^-$  is reduced by a factor  $2,000/350 \approx 6$ . Furthermore, from Table 4 one is tempted to deduce a  $1/p^2$  dependence of  $C(p)$  in separated beams, bringing in another improvement factor  $(8/5)^2 = 2.5$ .

Therefore it is concluded that the purity of an RF separated beam is improving quite rapidly between 5 and 8 GeV/c. The lower limit for satisfactory operation of RF separators in the O2 beam is higher than the 5 GeV/c assumed. It is rather somewhere between 7 and 8 GeV/c.

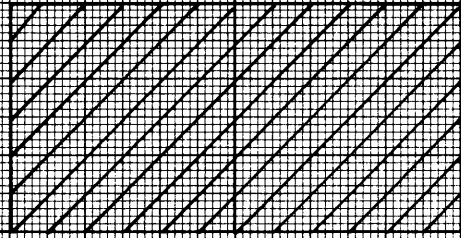
## 5. Acknowledgements

Thanks are due to J. Hornsby who kindly modified the original programme<sup>2)</sup> for the present application, and to Mlles. M. Hanney and Y. Jayet who did the numerical integrations and plotted the graphs.

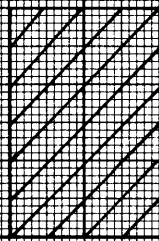
6. References

- 1) E. Keil, B. W. Montague, W. W. Neale, CERN/TC/NBC 62-2.
- 2) J. Fronteau, J. Hornsby, CERN 62-36 and private communication.
- 3) E. Keil, AR/Int. PSep./63-3.
- 4) E. Keil, AR/Int.PSep/63-6.
- 5) W. W. Neale, private communication.

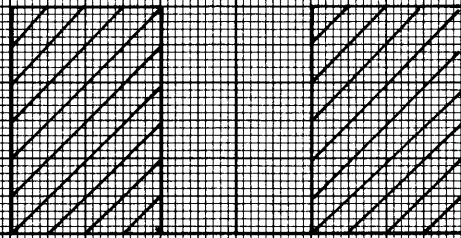




wide slit



narrow slit



beam stopper



Fig. 1

FIGURE 2

$p = 15 \text{ GeV}/c$  pion beam

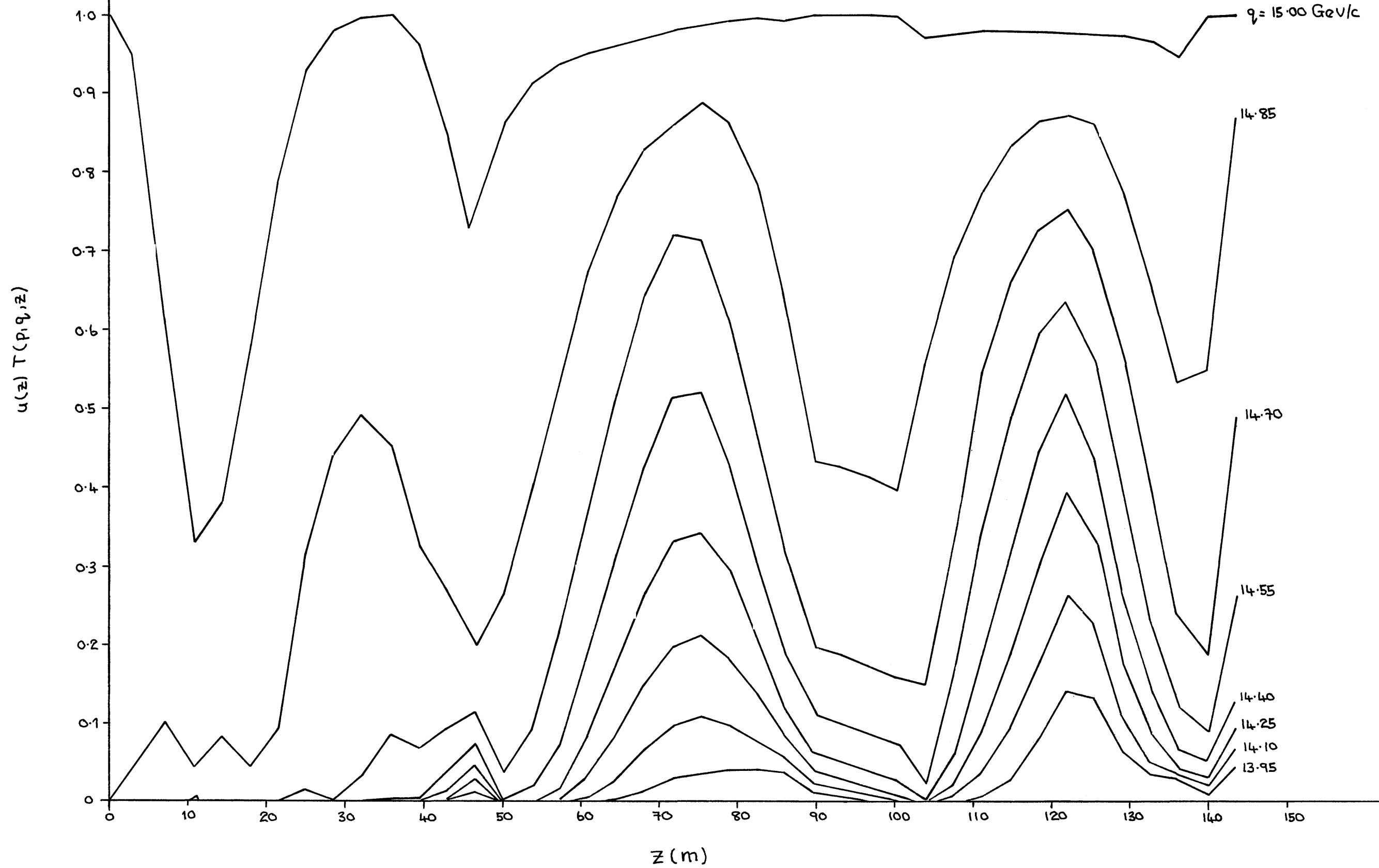
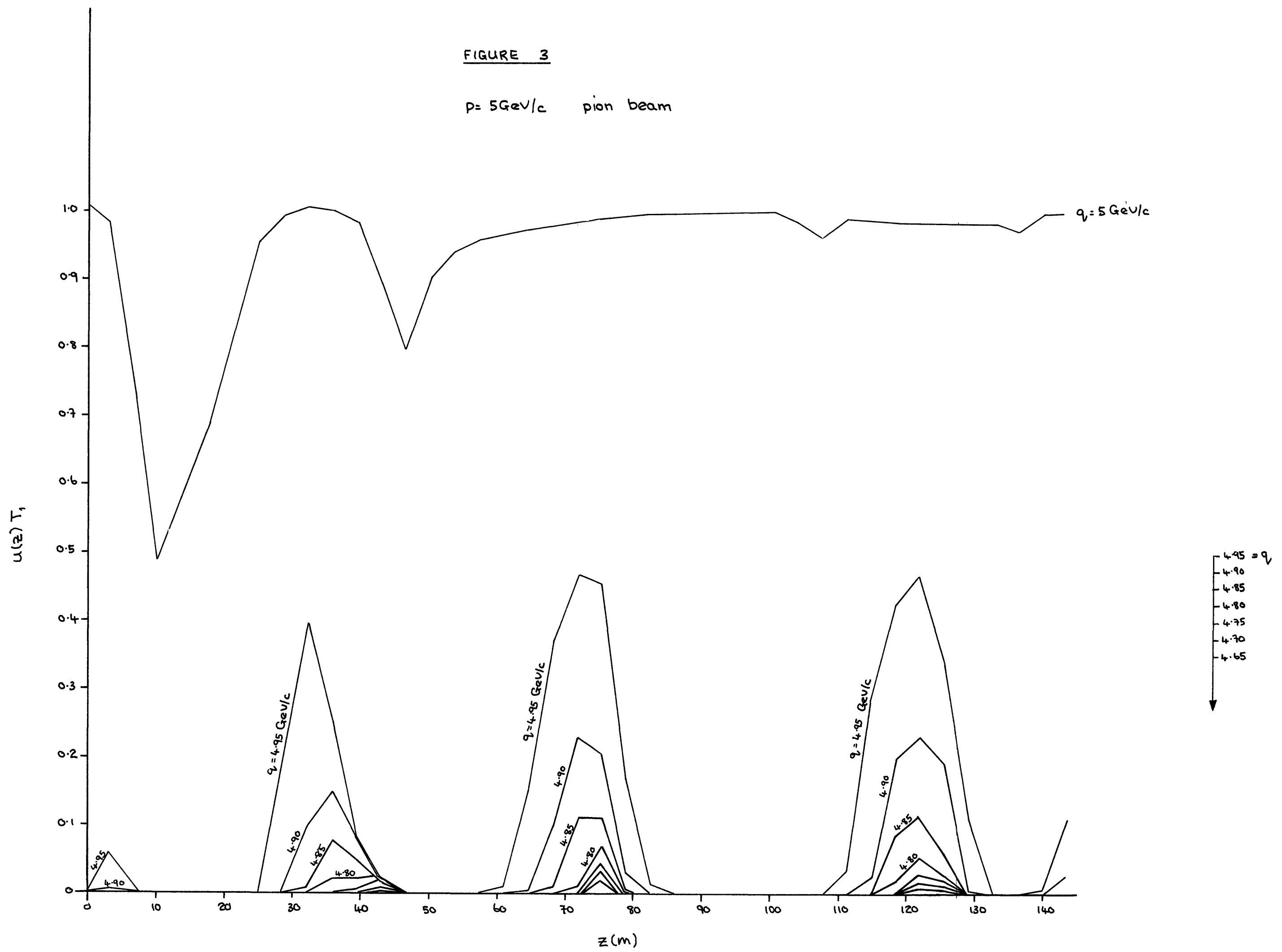


FIGURE 3

$p = 5 \text{ GeV}/c$  pion beam



$M(piq) [(GeV/c)^{-1}]$

$25 \times 10^{-3}$

Fig. 4

$p = 15 \text{ GeV}/c$

pion beam

20

15

10

5

0

13.5

14.0

14.5

15.0

$q [GeV/c]$

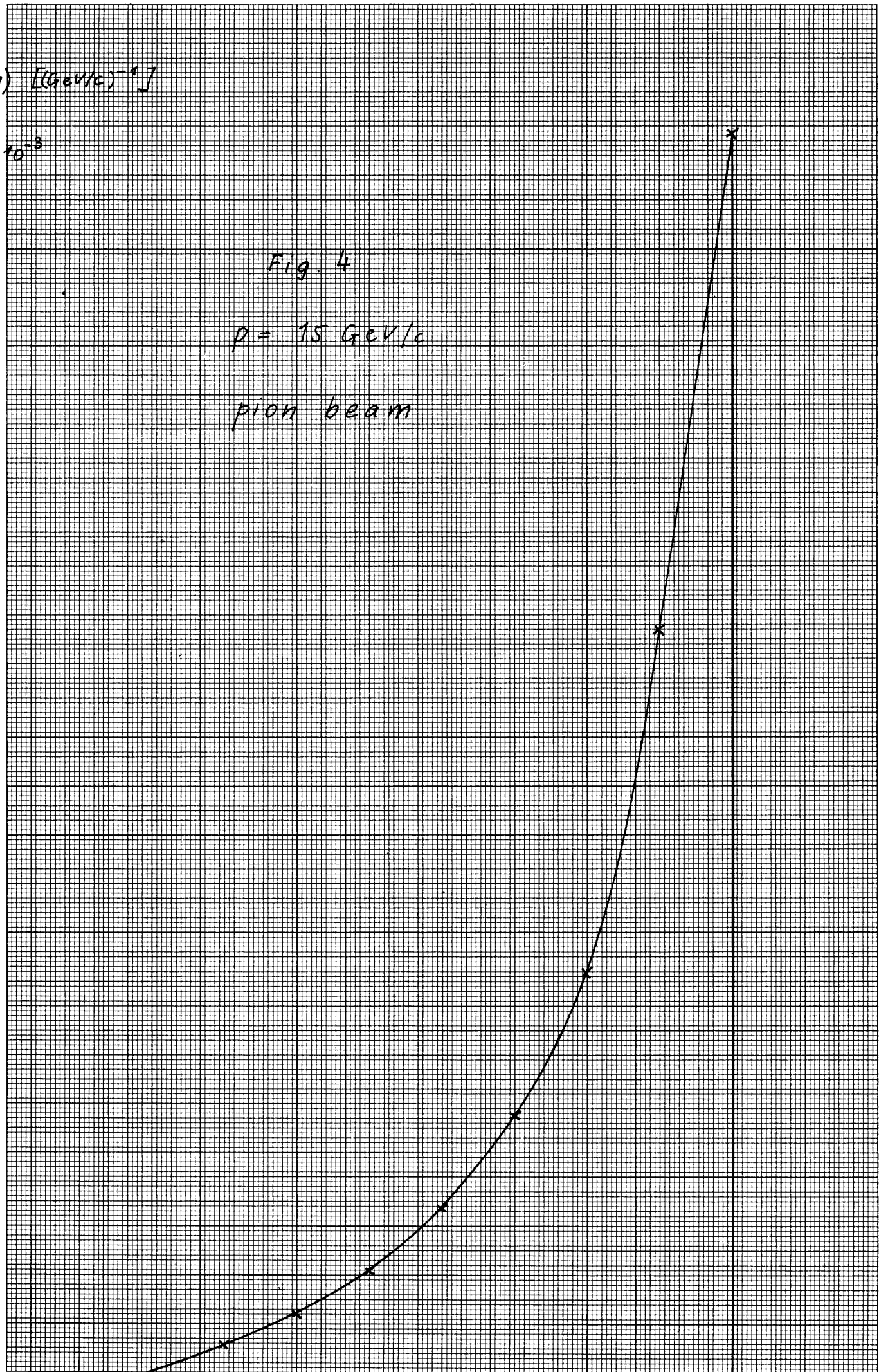


Fig. 5

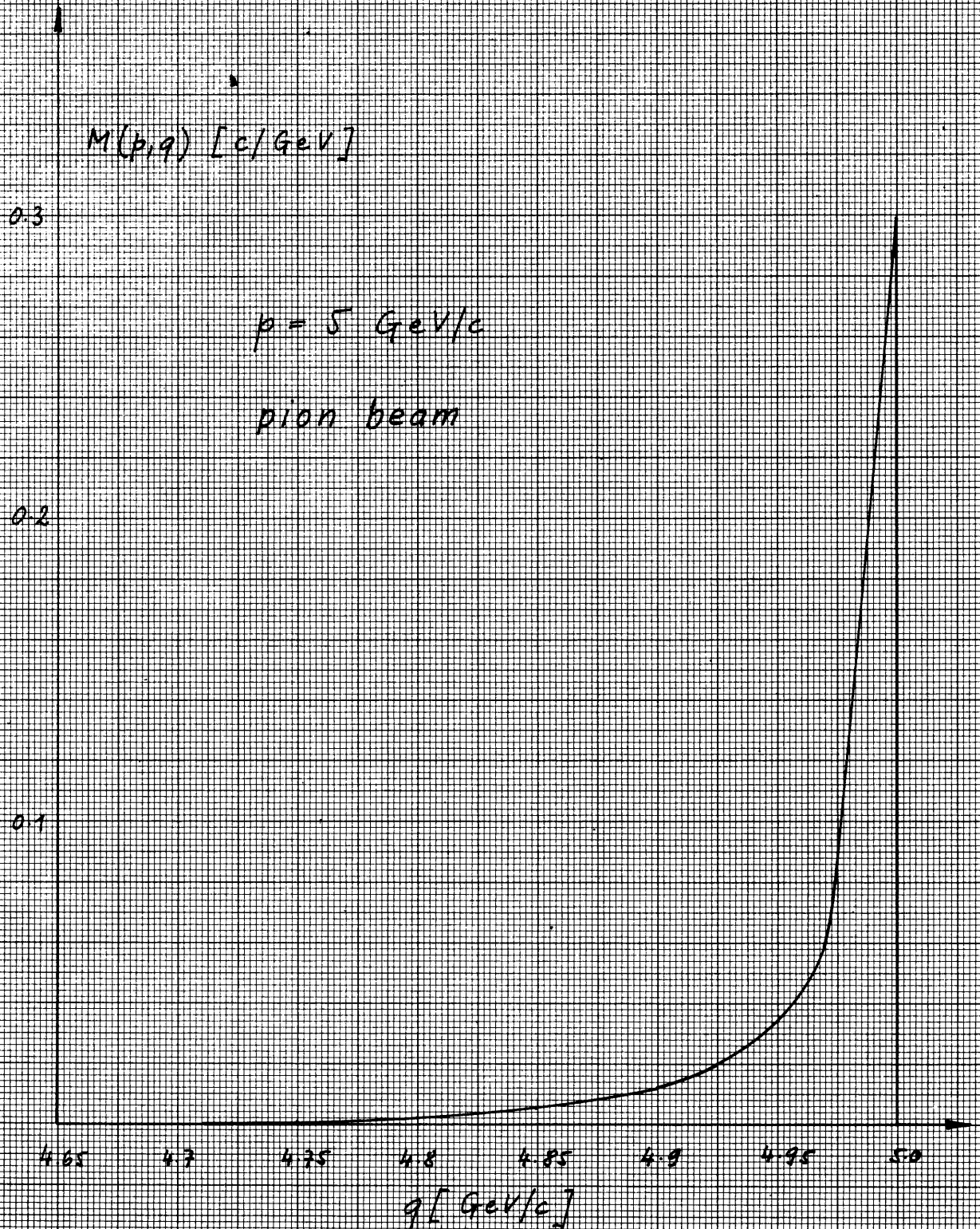


FIGURE 6a

$p = 15 \text{ GeV}/c$  separated beam

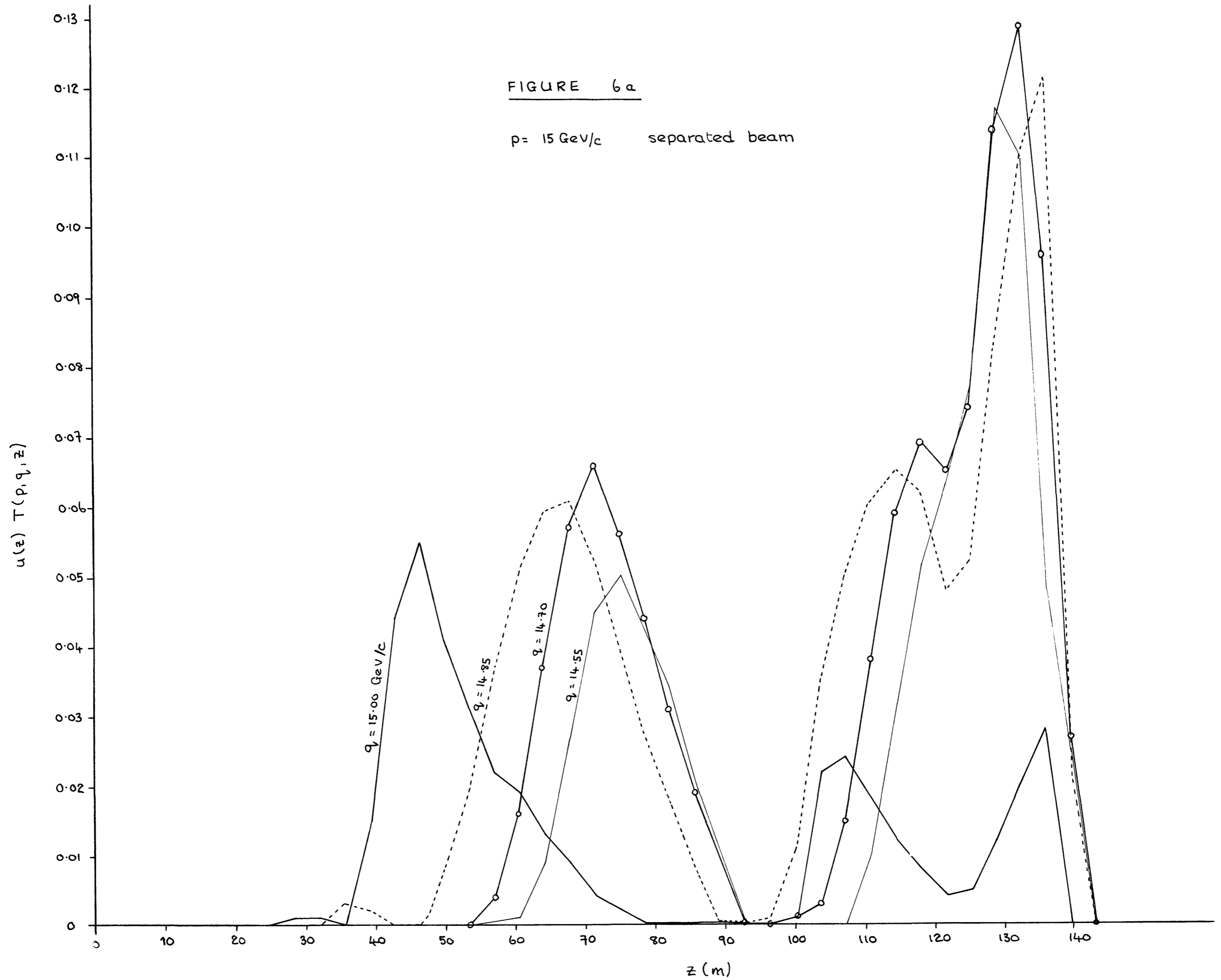


FIGURE 6b

$p = 15 \text{ GeV}/c$  separated beam

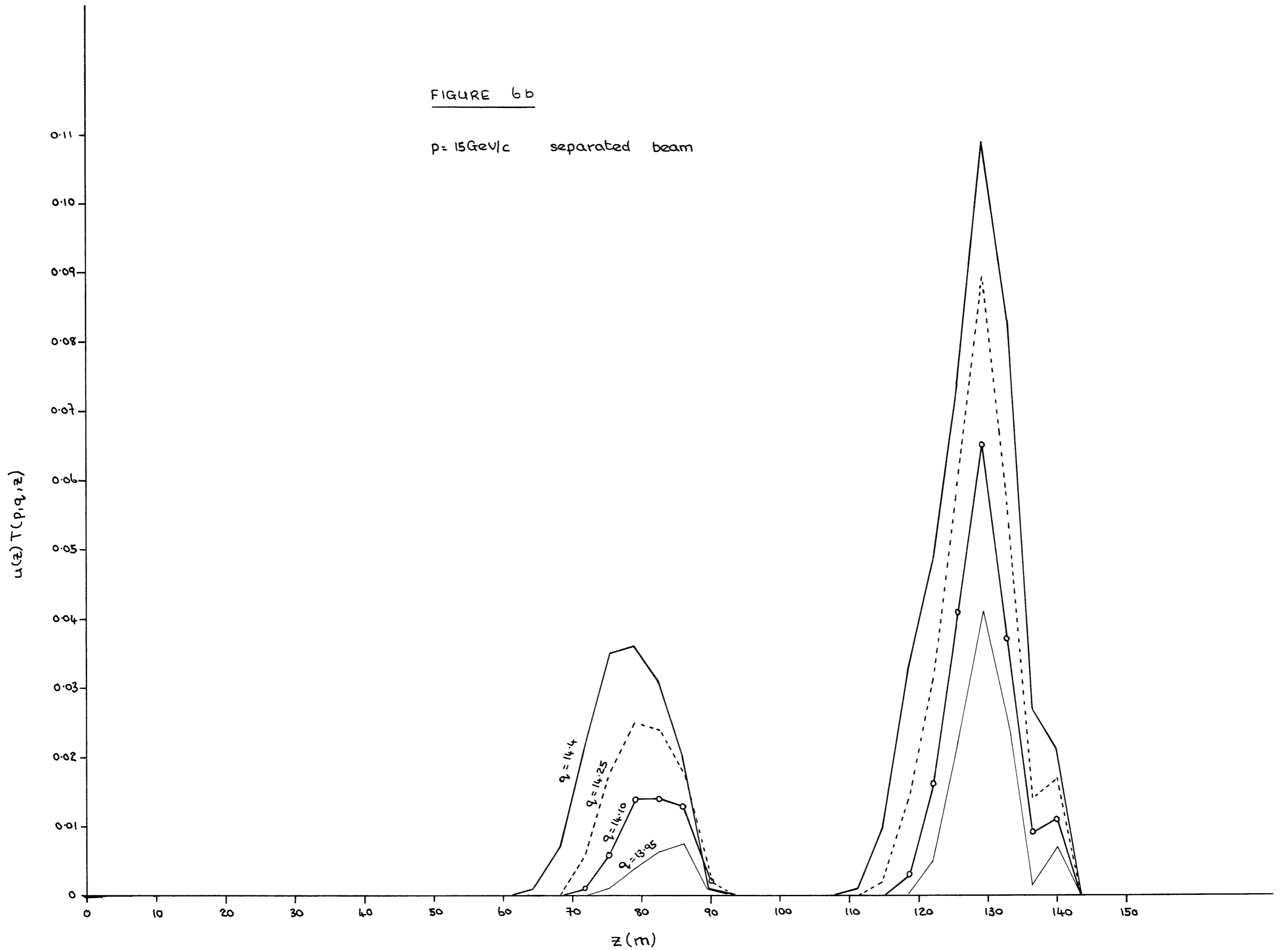


FIGURE 7a

p = 5 GeV/c      separated beam

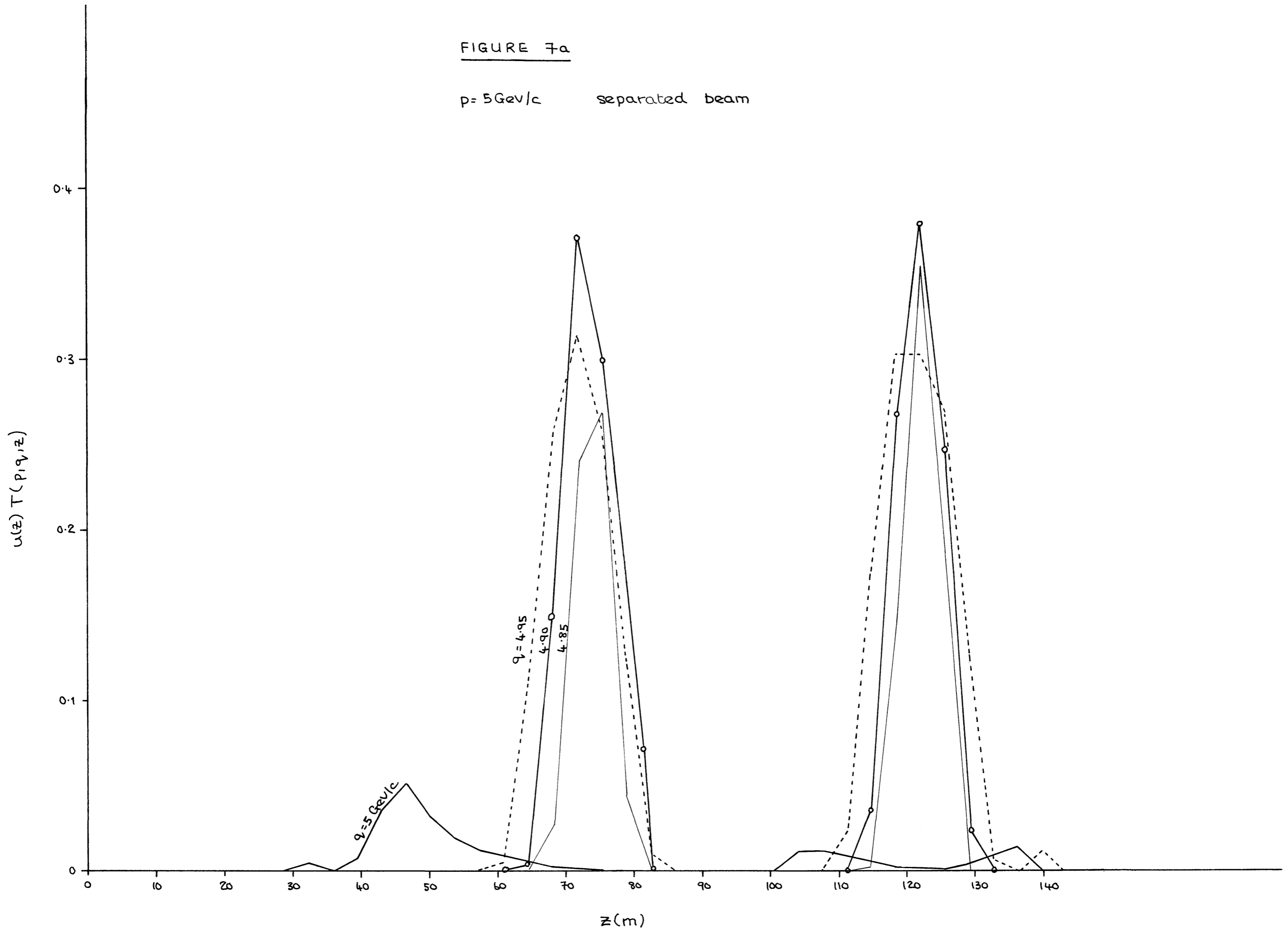




FIGURE 7b

$p = 5 \text{ GeV}/c$  separated beam

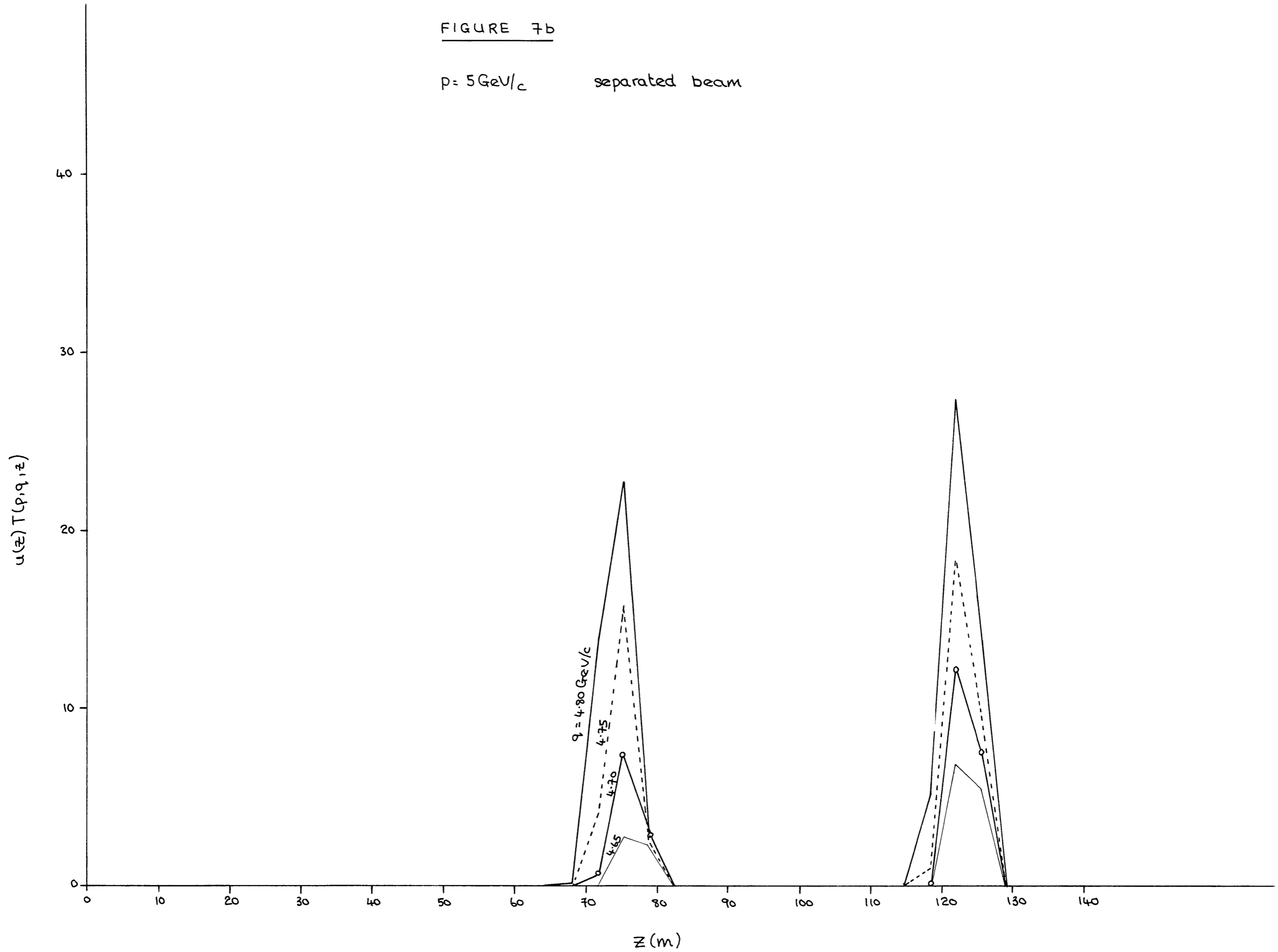


Fig. 8

$p = 15 \text{ GeV}/c$

separated beam

$M(p, q) \text{ [e/GeV]}$

$0.7 \times 10^{-3}$

0.6

0.5

0.4

0.3

0.2

0.1

0

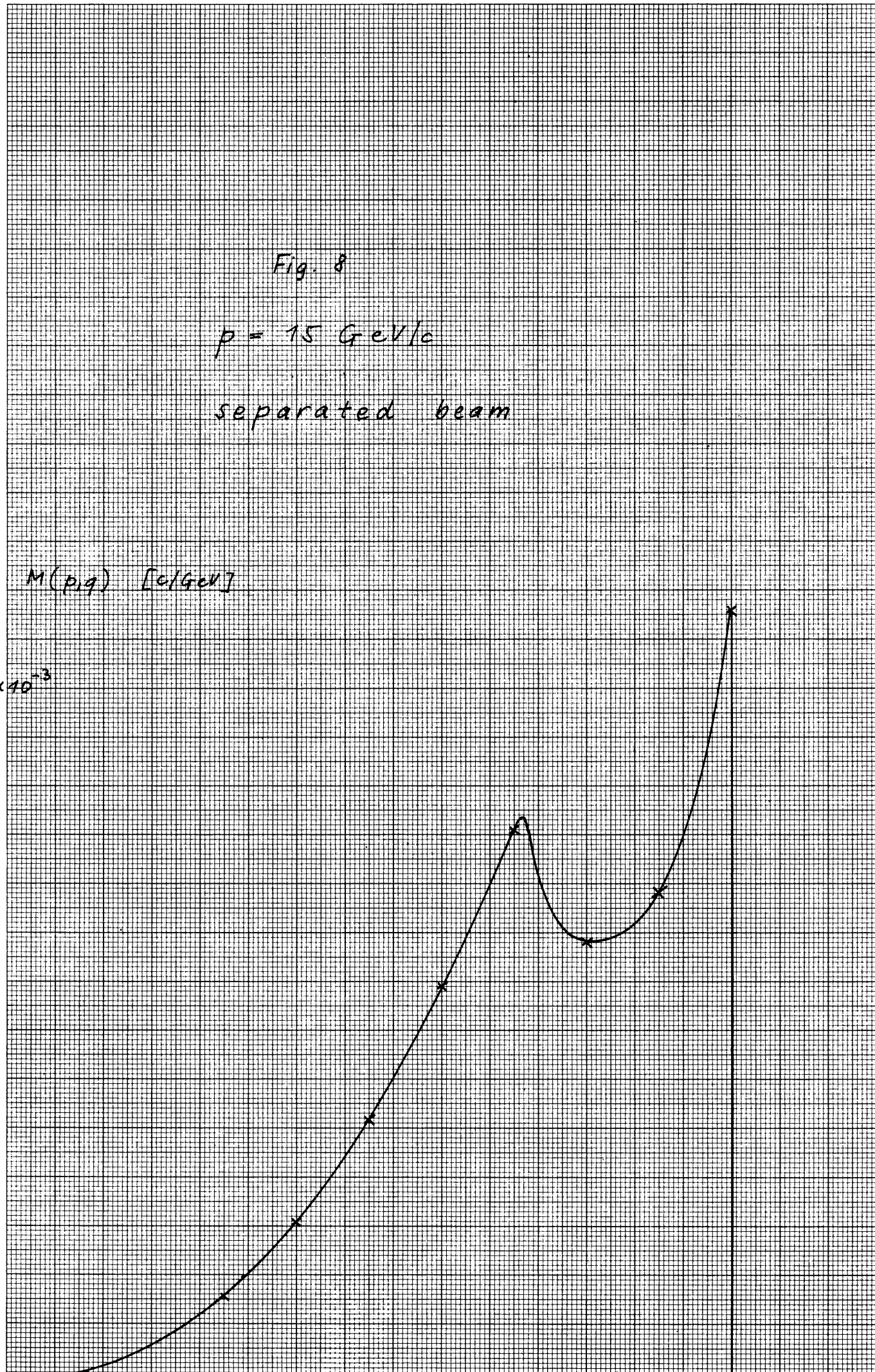
13.5

14.0

14.5

15.0

$q \text{ [GeV}/c]$



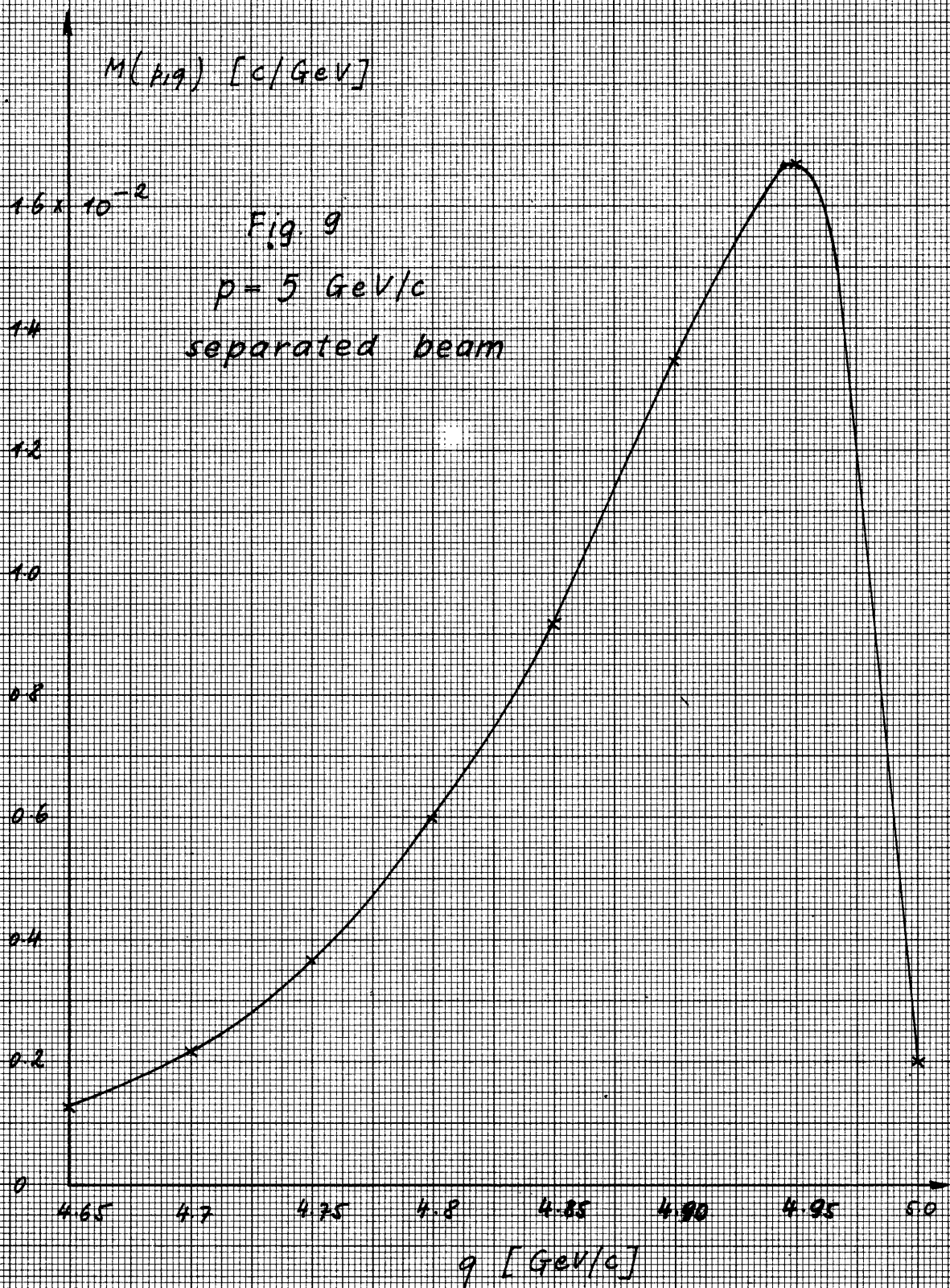
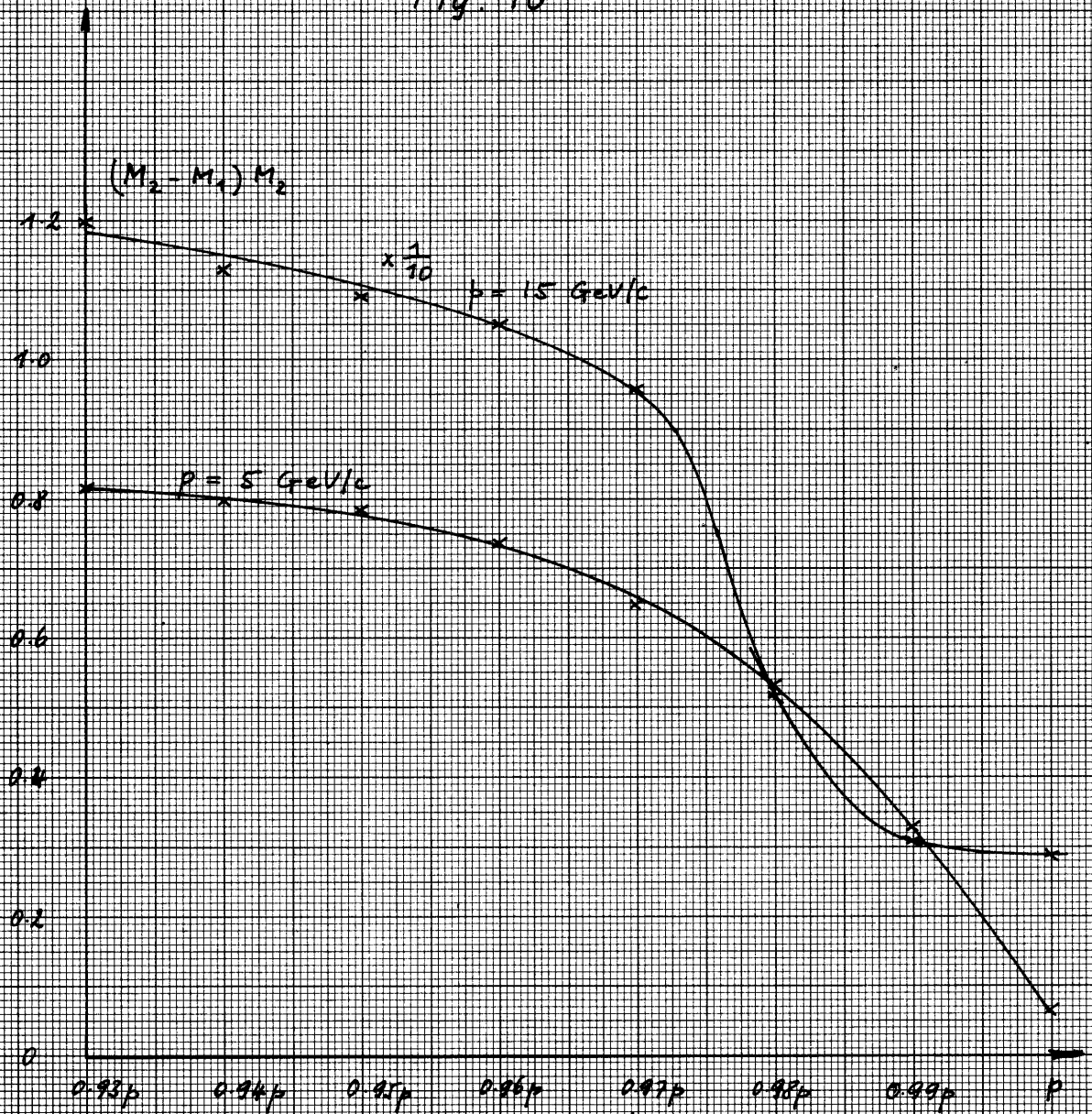


Fig. 10



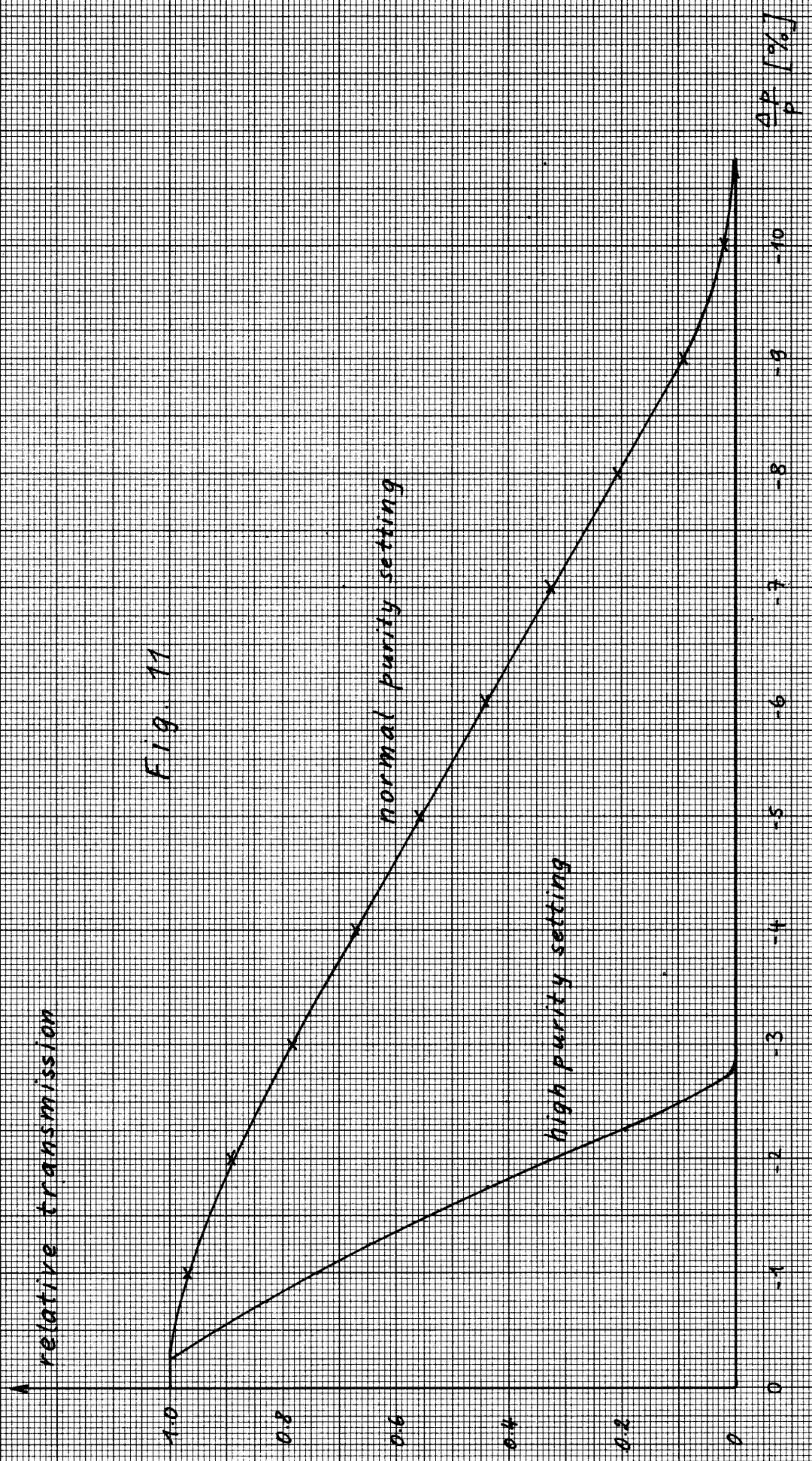


Fig. 11

